



Development of a Hybrid GAN Using CGAN and LS-Wasserstein Loss for Synthetic Data Generation in COVID-19 Severity Prediction

M. Ganiyu¹; O. Olabode²; O. C. Agbonifo³

¹Department of Computer Science, Federal Polytechnic, Ile-Oluji, Ondo State, Nigeria

²Department of Data Science, Federal University of Technology, Akure Ondo State, Nigeria

³Department of Information Systems, Federal University of Technology, Akure Ondo State, Nigeria

¹ mutganiyu@fedpolel.edu.ng; ² oolabode@futa.edu.ng; ³ ocagbonifo@futa.edu.ng

DOI: <https://doi.org/10.47760/ijcsmc.2025.v14i09.006>

Abstract: Development of a Hybrid GAN Using CGAN and LS-Wasserstein Loss for Synthetic Data Generation in COVID-19 Severity Prediction. To overcome the limitations of scarce and imbalanced chest X-ray data, three GAN variants CGAN, LS-GAN and WGAN were combined to develop a Hybrid GAN. 809 (538 COVID-19 and 271 Non-COVID-19) chest radiography images were obtained from the COVID-19 patient radiographic images and case note from the isolation centers of Nigeria hospital and GitHub repository. The CGAN, LS-GAN, WGAN and LS+W+CGAN were implemented to generate realistic, class-conditional synthetic images. The hybrid LS+W+CGAN achieved the best balance between training stability, visual fidelity, and diversity, producing high-quality synthetic images. The results showed that the hybridized GAN (LS+WS+CGAN) produced lowest D loss of -0.9784, FID of 372.56 and highest SSIM 0.3201 to achieve the best result compare to individual CGAN, LSGAN and WGAN.

Keywords: COVID-19 Severity Prediction, Conditional Generative Adversarial Networks (CGANs), Chest X-ray Imaging, Ensemble Machine Learning, Synthetic Data Augmentation

I. INTRODUCTION

COVID-19 is a highly contagious respiratory illness caused by the SARS-CoV-2 virus. The disease was first reported in Wuhan, China, in December 2019, after several pneumonia cases were linked to a seafood market. The virus is believed to have a zoonotic origin, possibly transmitted from bats to humans, though the exact pathway remains unclear [1]. By January 2020, human-to-human transmission was confirmed, and the virus began to spread rapidly worldwide. On March 11, 2020, the World Health Organization (WHO) declared COVID-19 a global pandemic due to its rapid spread and severe public health impact [2].

Early identification of infected individuals for prompt treatment and isolation to stop the disease's transmission are key components of an effective disease control strategy [3]. Effective management of illness propagation and treatment planning depend on early identification and study of infection patterns [4]. According to Lee *et al.* (2020), early screening for COVID-19 is essential to preventing the disease's spread and managing the limited medical resources because of the high infection rate, lack of effective therapy, and lack of proven vaccinations. 2019-CoV infection symptoms are comparable to those of SARS-CoV, with fever, dry cough, dyspnea, chest discomfort, exhaustion, and myalgia being the most prevalent symptoms [5,6]. Headache, nausea, vomiting, dizziness, abdominal discomfort, diarrhea, loss of taste and smell, and hemoptysis are less frequent symptoms [5].

Bilateral pneumonia affected over 75% of patients [7]. The fact that so few COVID-19 patients exhibit noticeable upper respiratory tract symptoms like rhinorrhea, sneezing, or sore throat differs from SARS-CoV and MERS-CoV infections, indicating that the virus may prefer to infect the lower respiratory tract [8]. Patients with COVID-19 have been documented to experience severe consequences, including shock, acute cardiac injury, acute renal injury, arrhythmia, hypoxemia, and acute ARDS [7,9]. COVID-19 spreads primarily through respiratory droplets, aerosols, and close personal contact. Common symptoms include fever, cough, fatigue, and shortness of breath, though asymptomatic cases are also common. Severe cases may result in pneumonia, acute respiratory distress syndrome (ARDS), or death, especially among the elderly and those with underlying conditions [10]. The clinical presentation ranges from asymptomatic infection to severe pneumonia, ARDS, and multi-organ failure, especially in elderly and immune-compromised individuals [8].

To control the pandemic, governments implemented lockdowns, travel restrictions, and public health measures. Rapid development and deployment of vaccines such as Pfizer-BioNTech, Moderna, and AstraZeneca have played a critical role in reducing severe disease and mortality [11]. Global initiatives such as COVAX were launched to ensure equitable vaccine distribution [12]. The diagnosis of COVID-19 involves several clinical and laboratory methods that help detect the presence of SARS-CoV-2, the virus responsible for the disease. Accurate and timely diagnosis is essential for isolating infected individuals, managing symptoms, and reducing the spread of the virus.

Researchers have recently focused on the augmentation of COVID-19 image datasets with synthetic data generated by Generative Adversarial Networks (GANs) to enhance machine learning performance in prediction and classification models. A GAN using deep learning was presented by Loey *et al.* (2020) in order to identify COVID-19 from chest X-rays [13]. GANs have found widespread applications in various domains. In computer vision, they are employed for image generation, image super-resolution, and style transfer. In healthcare, GANs assist in generating synthetic medical data to augment limited datasets. They are also utilized in natural language processing for text-to-image synthesis and in cybersecurity for generating adversarial examples [14].

II. LITERATURE REVIEW

A. History of COVID-19

The novel coronavirus disease 2019 (COVID-19) emerged in late 2019 in Wuhan, Hubei Province, China. It was first reported to the World Health Organization (WHO) on December 31, 2019, as a cluster of pneumonia cases with an unknown cause. The causative agent, later identified as Severe Acute Respiratory Syndrome Coronavirus 2 (SARS-CoV-2), is a novel strain of coronavirus not previously detected in humans [15]. Furthermore, COVID-19 is believed to have originated in a wet market in Wuhan, where live animals were sold, facilitating zoonotic transmission from animals to humans. However, the exact source of the virus remains under investigation. By January 2020, human-to-human transmission had been confirmed, leading to a rapid global spread of the virus [16].

On March 11, 2020, the WHO declared COVID-19 a global pandemic. This declaration underscored the rapid international spread and significant public health impact of the virus. Countries worldwide implemented various public health interventions, including lockdowns, travel restrictions, mask mandates, and mass vaccination campaigns to contain the virus and reduce mortality [2,17].

B. Methods of Detecting COVID-19

The detection of COVID-19, caused by the SARS-CoV-2 virus, is crucial for diagnosis, treatment, and controlling the spread of the disease. Various diagnostic techniques have been developed and widely deployed, each with specific advantages and limitations. These methods are broadly categorized into molecular tests, antigen tests, and serological tests [18].

I. Molecular Testing (RT-PCR)

The reverse transcription polymerase chain reaction (RT-PCR) test is the gold standard for detecting SARS-CoV-2. It detects viral RNA in respiratory specimens such as nasopharyngeal swabs, oropharyngeal swabs, and saliva. RT-PCR tests are highly sensitive and specific, often used in clinical and laboratory settings for confirming active infection [19].

II. Antigen Testing

Antigen tests detect specific viral proteins and are generally less sensitive than RT-PCR tests. They provide results more quickly, often within 15–30 minutes, making them useful for point-of-care settings and mass screening. However, their lower sensitivity may result in false negatives, particularly in asymptomatic individuals or those in early or late stages of infection [20].

III. Serological (Antibody) Testin

Serological tests detect antibodies (IgM, IgG) produced in response to SARS-CoV-2 infection. These tests are not used for diagnosing active infection but help determine past exposure and immune response. They are useful in epidemiological studies and in assessing population-level immunity [21].

IV. Emerging Diagnostic Methods

Recent advancements include the development of CRISPR-based diagnostic tools, loop-mediated isothermal amplification (LAMP), and next-generation sequencing (NGS). These methods promise improved accuracy, rapid detection, and broader accessibility, especially in resource-limited settings [22].

C. Machine Learning

Machine learning (ML) is a subfield of artificial intelligence (AI) that focuses on the development of algorithms and statistical models enabling computer systems to perform tasks without explicit instructions. Instead, these systems learn patterns from data and make decisions or predictions based on that data [23].

I. Supervised Learning

Models are trained using labeled data, allowing the algorithm to learn the mapping between inputs and outputs. Common applications include image classification, speech recognition, and medical diagnosis [24].

II. Unsupervised Learning

This involves training models on unlabeled data, where the algorithm identifies hidden patterns or intrinsic structures. It is commonly used in clustering, anomaly detection, and dimensionality reduction tasks such as customer segmentation and topic modeling [7].

III. Reinforcement Learning

In this type, an agent interacts with an environment and learns to make decisions by receiving rewards or penalties. Reinforcement learning has found success in robotics, game playing, and autonomous systems [25].

D. Generative Adversarial Networks (GANs)

Generative Adversarial Networks (GANs) are a class of machine learning models introduced by Ian Goodfellow and colleagues in 2014, designed to generate new, synthetic data samples that closely resemble a given training dataset. GANs have gained substantial attention in the fields of artificial intelligence and deep learning for their ability to produce highly realistic data, including images, videos, and audio [26].

The strength of GANs lies in their unsupervised learning paradigm. Unlike supervised models that require labeled data, GANs learn to generate data distributions without explicit annotations. This characteristic has made them highly valuable in domains where labeled data is scarce or costly to obtain [7]. Applications of GANs are vast and include image synthesis, super-resolution, image-to-image translation, data augmentation, 3D model generation, and even medical imaging enhancement. In addition to creative and commercial uses, GANs are also used for scientific simulations and anomaly detection [27].

However, GANs are not without challenges. They are known for training instability, mode collapse (where the generator produces limited varieties of outputs), and sensitivity to hyperparameters. Significant research efforts continue to address these limitations and improve the robustness and efficiency of GAN training processes [28].

III. METHODOLOGY

Data Source and Description

Data was obtained from the COVID-19 patient radiographic images and case note from the isolation centers of Nigeria hospital and GitHub repository. The original dataset contained 809 (538 COVID-19 and 271 Non-COVID-19) chest radiography images while 2400 (1200 COVID-19 and 1200 Non-COVID-19) chest radiography synthetic images were generated.

Hybridizing Conditional GAN, Least-Squares and Wasserstein

Hybridizing CGAN, LS and Wasserstein provides the model that benefits from conditional control, strong gradient signals, and stable global distribution matching.

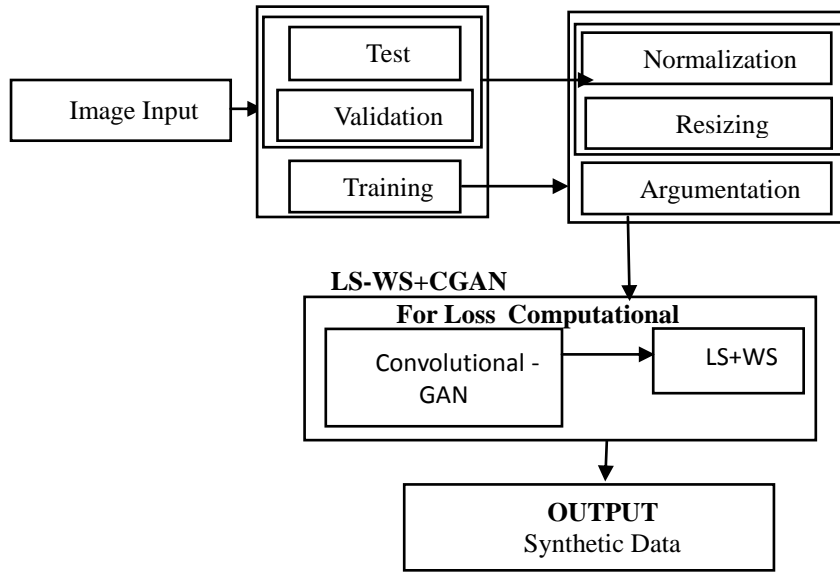


Figure 1: Conceptualized Framework for the System

Procedures of Hybridizing CGAN, Least-Squares and Wasserstein

Conditional GANs extend the traditional GAN architecture by conditioning both the generator and discriminator on auxiliary information, such as class labels. Instead of only learning to generate realistic samples, CGANs also learn to generate samples conditioned on external information c , such as class labels, attributes, or text. CGAN is defined as $G(z, c)$ and $D(x, c)$.

Generator (G): Inputs *random noise* z and *condition vector* c and *concatenate* both at the input layer. It carries out conditional batch normalization within hidden layers and generate sample $G(z, c)$ that match the target class as output.

Discriminator (D): Shared feature extractor (backbone) followed by two heads which are:

- i. **Wasserstein critic head** $D_w(x, c)$ which produces unbounded scalar score for real or fake distribution.
 - ii. **Least Squares head** $D_{ls}(x, c)$ which outputs scalar to compare with target labels (real ≈ 1 , fake ≈ 0).
- Condition vector c is injected via concatenation

Loss Function Mathematical Model

i. Least Square GAN Loss

To improve stability and mitigate the vanishing gradient problem in CGAN, the Least Squares GAN (LSGAN) is incorporated. Instead of using the standard binary cross-entropy loss, LSGAN minimizes the Pearson χ^2 divergence by penalizing samples based on their squared distance from the decision boundary.

$$\text{Generator LS loss: } L_G^{LS} = \frac{1}{2} E_{x \sim P_y} [(D_{ls}(x, c) - 1)^2] \quad (i)$$

$$\text{Discriminator LS loss: } L_D^{LS} = \frac{1}{2} E_{x \sim P_{data}} [(D_{ls}(x, c) - 1)^2] + \frac{1}{2} E_{x \sim P_y} [(D_{ls}(x, c) - 1)^2] \quad (ii)$$

ii. WGAN-GP Loss (critic)

To further address issues of training instability, the Wasserstein GAN (WGAN) framework was adopted. WGAN replaces the discriminator with a critic that estimates the Earth Mover’s distance between real and generated distributions. The loss function is given by:

$$\text{Generator: } \mathcal{L}_G^W = -\mathbb{E}_{x \sim p_g} [D_w(x, c)] \tag{iii}$$

$$\text{Discriminator: } \mathcal{L}_D^W = \mathbb{E}_{x \sim p_g} [D_w(x, c)] - \mathbb{E}_{x \sim p_{\text{data}}} [D_w(x, c)] + \lambda_{\text{gp}} \mathbb{E}_{\hat{x} \sim p_{\hat{x}}} [(\|\nabla_{\hat{x}} D_w(\hat{x}, c)\|_2 - 1)^2] \tag{iv}$$

iii. Combined Loss (Hybrid)

The core novelty of this work lies in the hybridized LS+WS + CGAN model, which combines the advantages of LSGAN, WGAN, and CGAN. By integrating least squares and Wasserstein objectives into the conditional framework, the hybrid model leverages stable training (LSGAN), improved gradient quality (WGAN), and label conditioning (CGAN). The combined loss is expressed as:

$$\text{Generator: } \mathcal{L}_G = \lambda_w \mathcal{L}_G^W + \lambda_{ls} \mathcal{L}_G^{LS} \tag{v}$$

$$\text{Discriminator: } \mathcal{L}_D = \lambda_w \mathcal{L}_D^W + \lambda_{ls} \mathcal{L}_D^{LS} \tag{vi}$$

where

λ_w, λ_{ls} balance the influence of WGAN and LSGAN components.

IV. RESULT

This section presents the results of experiments conducted using Conditional Generative Adversarial Networks (CGANs) to generate synthetic COVID-19 severity data for improved training of classification models. Different loss functions were evaluated, including Least Squares Loss (LS-CGAN), Wasserstein Loss (W-CGAN), and a Hybrid Loss (LS+W-CGAN).

A. CGAN Realism Test

An initial realism test was performed to evaluate the quality of synthetic images generated by the CGAN framework. The test involved both subjective visual inspection and objective evaluation of generated outputs across severity classes.

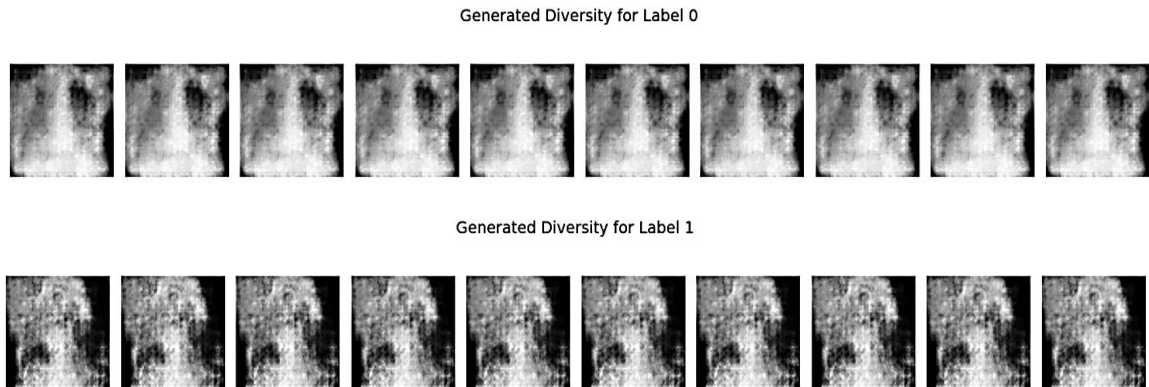
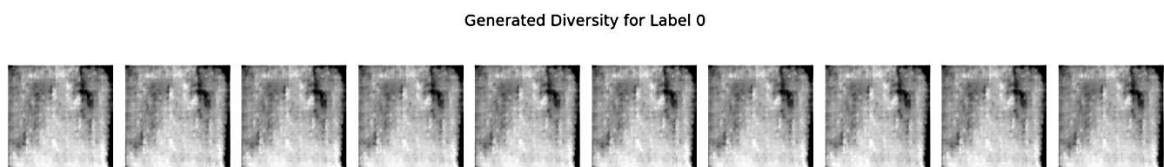


Figure 2 CGAN realism test results.

As shown in Figure 2, the realism test demonstrates that the CGAN was able to produce class-consistent samples. Although the outputs captured key features of the underlying dataset, some generated images exhibited artifacts and lacked fine detail.

B. LS-CGAN Results

The LS-CGAN employed the least squares loss to stabilize training and mitigate vanishing gradient issues. The generated outputs were visually consistent but showed evidence of mode collapse in certain classes.



Generated Diversity for Label 1

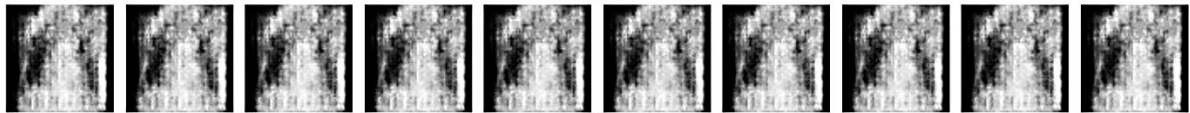


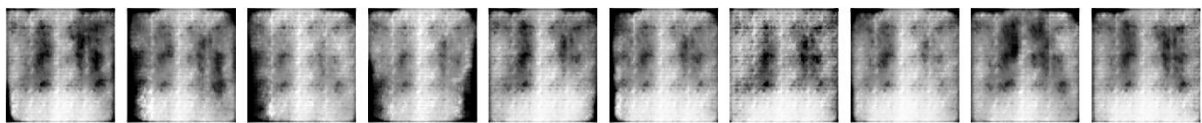
Figure 3: Realism test for LS-CGAN.

Figure 3 confirms that while LS-CGAN achieved moderate realism, it underperformed compared to subsequent model, with images appearing less sharp and occasionally distorted.

C. W-CGAN Results

The W-CGAN utilized the Wasserstein distance to improve convergence and reduce training instabilities. This model produced sharper and more realistic images compared to LS-CGAN, although fluctuations in loss curves indicated instability.

Generated Diversity for Label 0



Generated Diversity for Label 1

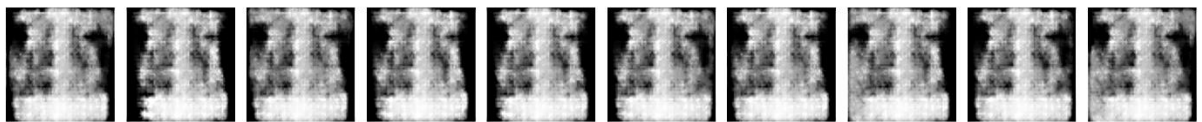


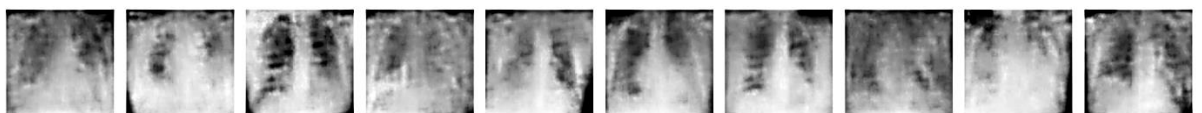
Figure 4: Realism test for W-CGAN.

Figure 4 illustrates the realism test results, where W-CGAN demonstrated higher reliability in producing sharp images, but occasional instability during training was observed.

D. Hybrid LS+W-CGAN Results

To combine the advantages of LS and Wasserstein losses, a hybrid LS+W-CGAN was implemented. This hybrid model achieved the best trade-off between training stability, image sharpness, and diversity.

Generated Diversity for Label 0



Generated Diversity for Label 1

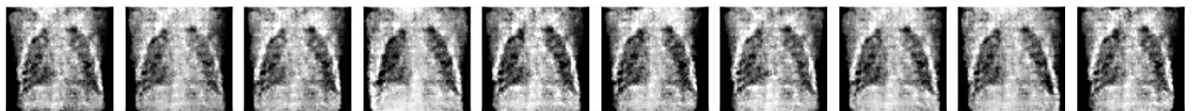


Figure 5: Realism test for Hybrid LS+W-CGAN.

Figure 4.7 highlights the realism test results, where Hybrid LS+W-CGAN demonstrated superior visual fidelity.

E. Quantitative Evaluation

To complement the qualitative findings, quantitative metrics were computed for each model. These included Discriminator Loss (D-Loss), Generator Loss (G-Loss), Structural Similarity Index Measure (SSIM), and Frechet Inception Distance (FID). Table 1 summarizes the results.

Table 1: Quantitative evaluation of CGAN models

Model	D-Loss	G-Loss	SSIM	Average FID
CGAN	0.5543	1.2750	0.1882	412.44
LS-CGAN	0.1874	0.4510	0.2099	414.26
W-CGAN	-1.2597	-1.9390	0.2481	408.80
LS+W-CGAN	-0.9784	2.3359	0.3201	372.56

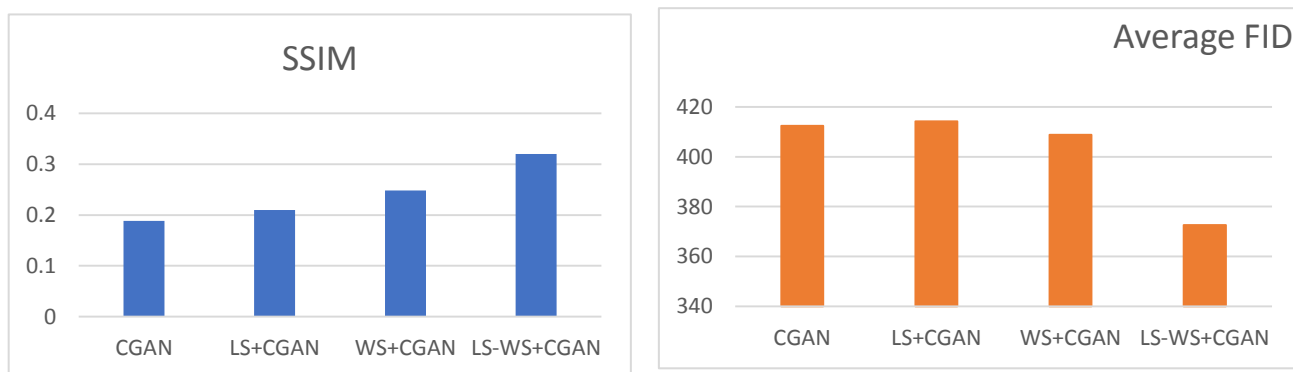


Figure 6: Comparison of the models performance using SSIM and FID

Interpretation of Results

I. Loss Values (D-Loss and G-Loss)

LS-CGAN achieved relatively low loss magnitudes, but this did not translate into superior realism. W-CGAN produced negative losses, which is expected in the Wasserstein framework, while the Hybrid LS+W-CGAN exhibited a balanced discriminator performance despite higher generator loss—consistent with improved diversity.

II. SSIM

SSIM values confirmed structural similarity trends. The baseline CGAN performed the worst (0.1882), while LS+W-CGAN achieved the highest score (0.3201), indicating superior structural fidelity.

III. FID

Lower FID values reflect closer alignment between real and synthetic data distributions. LS+W-CGAN attained the lowest FID (372.56), clearly outperforming the other variants. LS-CGAN, in contrast, slightly worsened performance compared to the baseline CGAN.

V. CONCLUSIONS

This research has introduced a hybridized Conditional Generative Adversarial Network (CGAN) enhanced with Least Squares and Wasserstein loss functions to generate realistic synthetic chest X-ray images for COVID-19 diagnosis and severity level prediction. The hybridized GAN (LS+WS+CGAN) produced lowest D loss of -0.9784, FID of 372.56 and highest SSIM 0.3201 to achieve the best result compare to individual CGAN, LSGAN and WGAN.

REFERENCES

- [1] P. Zhou et al., “A pneumonia outbreak associated with a new coronavirus of probable bat origin,” *Nature*, vol. 579, pp. 270–273, 2020.
- [2] World Health Organization, “WHO Director-General’s opening remarks at the media briefing on COVID-19—11 March 2020,” 2020. [Online]. Available: <https://www.who.int/director-general/speeches/detail/who-director-general-s-opening-remarks-at-the-media-briefing-on-covid-19---11-march-2020>
- [3] S. Wang et al., “A deep learning algorithm using CT images to screen for COVID-19,” *medRxiv*, 2020, doi: 10.1101/2020.02.14.20023022.

- [4] M. A. Khan, M. Alhaisoni, A. Tariq, M. N. Al-Sahaf, A. A. Albeshier, and H. Abdalla, “A robust hybrid deep learning features and ensemble learning algorithm for COVID-19 classification using chest X-ray images,” *Comput. Biol. Med.*, vol. 141, p. 105157, 2022.
- [5] R. Girshick, “Fast R-CNN,” in *Proc. IEEE Int. Conf. Comput. Vis. (ICCV)*, 2015, pp. 1440–1448.
- [6] X. Xu *et al.*, “Imaging and clinical features of patients with 2019 novel coronavirus,” *Eur. J. Nucl. Med. Mol. Imaging*, vol. 47, pp. 1022–1023, 2020.
- [7] H. Mohammad-Rahimi, M. Nadimi, M. H. Rohban, E. Shamsoddin, and S. E. Lee, “Application of machine learning in diagnosis of COVID-19 through X-ray and CT images: a scoping review,” *Front. Cardiovasc. Med.*, vol. 8, p. 638011, 2021.
- [8] C. Huang *et al.*, “Clinical features of patients infected with 2019 novel coronavirus in Wuhan, China,” *Lancet*, vol. 395, no. 10223, pp. 497–506, 2020.
- [9] Y. Song *et al.*, “Deep learning enables accurate diagnosis of novel coronavirus (COVID-19) with CT images,” *IEEE/ACM Trans. Comput. Biol. Bioinf.*, vol. 18, no. 6, pp. 2775–2780, 2021.
- [10] Centers for Disease Control and Prevention, “Symptoms of COVID-19,” CDC, 2020. [Online]. Available: <https://www.cdc.gov/coronavirus/2019-ncov/symptoms-testing/symptoms.html>
- [11] F. P. Polack *et al.*, “Safety and efficacy of the BNT162b2 mRNA Covid-19 vaccine,” *N. Engl. J. Med.*, vol. 383, no. 27, pp. 2603–2615, 2020.
- [12] World Health Organization, “COVAX,” 2020. [Online]. Available: <https://www.who.int/initiatives/accelerator/covax>
- [13] M. Loey, G. Manogaran, M. H. N. Taha, and N. E. M. Khalifa, “A hybrid deep transfer learning model with machine learning methods for COVID-19 chest X-ray classification using GAN,” *Alex. Eng. J.*, vol. 60, no. 1, pp. 365–377, 2021.
- [14] A. Creswell *et al.*, “Generative adversarial networks: An overview,” *IEEE Signal Process. Mag.*, vol. 35, no. 1, pp. 53–65, 2018.
- [15] World Health Organization, “Overview of Testing for SARS-CoV-2 (COVID-19),” 2023. [Online]. Available: <https://www.cdc.gov/coronavirus/2019-ncov/hcp/testing-overview.html>
- [16] J. T. Wu, K. Leung, and G. M. Leung, “Nowcasting and forecasting the potential domestic and international spread of the 2019-nCoV outbreak originating in Wuhan, China: A modelling study,” *Lancet*, vol. 395, no. 10225, pp. 689–697, 2020.
- [17] Centers for Disease Control and Prevention, “Public Health Interventions for COVID-19,” CDC, 2021. [Online]. Available: <https://www.cdc.gov/coronavirus/2019-ncov/php/public-health-interventions.html>
- [18] Centers for Disease Control and Prevention, “Overview of Testing for SARS-CoV-2 (COVID-19),” CDC, 2023. [Online]. Available: <https://www.cdc.gov/coronavirus/2019-ncov/hcp/testing-overview.html>
- [19] World Health Organization, “Recommendations for national SARS-CoV-2 testing strategies and diagnostic capacities,” 2021/2022. [Online]. Available: <https://www.who.int/publications/i/item/WHO-2019-nCoV-lab-testing-2021.1-eng>
- [20] U.S. Food and Drug Administration, “At-Home OTC COVID-19 Diagnostic Tests,” FDA, 2023. [Online]. Available: <https://www.fda.gov/medical-devices/coronavirus-covid-19-and-medical-devices/home-otc-covid-19-diagnostic-tests>
- [21] F. Krammer and V. Simon, “Serology assays to manage COVID-19,” *Science*, vol. 368, no. 6495, pp. 1060–1061, 2020.
- [22] J. S. Chen *et al.*, “CRISPR-Cas12a-assisted rapid and sensitive detection of SARS-CoV-2,” *Nat. Biomed. Eng.*, vol. 5, pp. 1228–1235, 2021.
- [23] T. M. Mitchell, *Machine Learning*. New York, NY, USA: McGraw-Hill, 1997.
- [24] J. D. Kelleher, B. Mac Namee, and A. D’Arcy, *Fundamentals of Machine Learning for Predictive Data Analytics: Algorithms, Worked Examples, and Case Studies*. Cambridge, MA, USA: MIT Press, 2015.
- [25] R. S. Sutton and A. G. Barto, *Reinforcement Learning: An Introduction*, 2nd ed. Cambridge, MA, USA: MIT Press, 2018.
- [26] I. J. Goodfellow *et al.*, “Generative adversarial nets,” in *Proc. Adv. Neural Inf. Process. Syst. (NeurIPS)*, 2014, pp. 2672–2680.
- [27] Z. Pan, W. Yu, X. Yi, A. Khan, F. Yuan, and Y. Zheng, “Recent progress on generative adversarial networks (GANs): A survey,” *IEEE Access*, vol. 7, pp. 36322–36333, 2019.
- [28] M. Lucic, K. Kurach, M. Michalski, S. Gelly, and O. Bousquet, “Are GANs created equal? A large-scale study,” in *Proc. Adv. Neural Inf. Process. Syst. (NeurIPS)*, 2018, pp. 698–707.